

Regulation of Polyp-to-Jellyfish Transition in *Aurelia aurita*

Björn Fuchs,^{1,5,7} Wei Wang,^{1,7} Simon Graspeuntner,¹ Yizhu Li,¹ Santiago Insua,¹ Eva-Maria Herbst,¹ Philipp Dirksen,¹ Anna-Marei Böhm,¹ Georg Hemmrich,² Felix Sommer,⁴ Tomislav Domazet-Lošo,³ Ulrich C. Klostermeier,² Friederike Anton-Erxleben,¹ Philip Rosenstiel,² Thomas C.G. Bosch,¹ and Konstantin Khalturin^{1,6,8,*}

¹Zoologisches Institut, Christian-Albrechts-Universität zu Kiel, Am Botanischen Garten 1–9, 24118 Kiel, Germany

²Institut für Klinische Molekularbiologie, Universitätsklinikum Schleswig-Holstein, Schittenhelmstrasse 12, 24105 Kiel, Germany

³Institut Ruder Bošković, Bijenička cesta 54, 10000 Zagreb, Croatia

⁴Wallenberg Laboratory for Cardiovascular and Metabolic Research, Sahlgrenska University Hospital, University of Gothenburg, 413 45 Gothenburg, Sweden

⁵Leica Microsystems AG, Max Schmidheiny Strasse 201, 9435 Heerbrugg, Switzerland

⁶Department of Invertebrate Zoology, Saint Petersburg State University, Universitetskaya naberezhnaya 7/9, 199034 Saint Petersburg, Russia

Summary

Background: The life cycle of scyphozoan cnidarians alternates between sessile asexual polyps and pelagic medusa. Transition from one life form to another is triggered by environmental signals, but the molecular cascades involved in the drastic morphological and physiological changes remain unknown.

Results: We show in the moon jelly *Aurelia aurita* that the molecular machinery controlling transition of the sessile polyp into a free-swimming jellyfish consists of two parts. One is conserved and relies on retinoic acid signaling. The second, novel part is based on secreted proteins that are strongly upregulated prior to metamorphosis in response to the seasonal temperature changes. One of these proteins functions as a temperature-sensitive “timer” and encodes the precursor of the strobilation hormone of *Aurelia*.

Conclusions: Our findings uncover the molecule framework controlling the polyp-to-jellyfish transition in a basal metazoan and provide insights into the evolution of complex life cycles in the animal kingdom.

Introduction

In humans, one genome corresponds to only one body plan. Among metazoans, this is more the exception than the rule. In the majority of animal taxa, one genome encodes several life forms that follow each other during ontogeny. A life cycle, accordingly, includes one or several drastic transformations of

a body plan, termed metamorphosis. Classic examples of bilaterians with complex life cycles are insects and amphibians, in which the molecular machinery of metamorphosis has been intensively studied. In both groups, the transition between life stages is tightly regulated by the neuronal and hormonal signals, which are integrated at the level of nuclear hormone receptors (EcR, TR, USP, and RxR) that activate the metamorphosis-specific genes [1–3]. Outside of arthropods and chordates, our knowledge of molecular pathways responsible for metamorphosis remains fragmented. For the prevailing majority of the invertebrate taxa, neither the metamorphosis hormones nor the molecular cascades responsible for life-cycle regulation are known.

Cnidarians represent one of the most basal animal groups in which complex life cycles are present (Figure 1A). Their phylogenetic position provides an opportunity to explore the ancestral characteristics of the life-cycle regulation machinery. The life cycle of Medusozoa (Hydrozoa, Cubozoa, and Scyphozoa) consists of two morphologically disparate generations with three well-defined life stages—planula larvae, polyp, and jellyfish (Figure 1B). Transition from one stage into another is tightly regulated by environmental stimuli and depends on seasonal rhythms [4–7]. In corals and sea anemones (Anthozoa), a life cycle consisting only of planula and polyp stages is common [8, 9].

Cnidarian life-cycle evolution has been debated for more than 100 years [9, 10], but so far its regulation is only poorly understood at the molecular level. The only known molecule with life-cycle regulatory potential is a neuropeptide, LWamide, that induces larva-to-polyp transition in the hydrozoan *Hydractinia echinata* [11]. Besides that, retinoids have been reported to influence the metamorphosis of polyps in *Hydractinia* [12], and a retinoic acid X receptor (jRxR) with a remarkable homology to vertebrate retinoic X receptors (RxRs) has been isolated from cubozoan *Tripedalia cystophora* [13]. Recently, the anti-inflammatory drug indomethacin was reported by Kuniyoshi and colleagues to be a potent inducer of polyp-to-jellyfish transition in *Aurelia* [14]. However, the reason for its function has remained obscure. Thus, despite a long history of studies and several important findings mentioned above, genetic regulation of a metagenetic life cycle remains enigmatic.

In order to elucidate the molecular machinery of metamorphosis in the basal Metazoa, we investigated the polyp-to-jellyfish transition, termed strobilation, in the moon jelly *Aurelia aurita* (Figure 1B). In nature, strobilation in *Aurelia* is a seasonal process that starts in winter or early spring [7, 15]. Most probably, the winter decrease in water temperature serves as an environmental cue perceived by the polyps. In laboratory conditions, similar to that in nature, metamorphosis can be induced by lowering the water temperature by several degrees (Figure 1C) [6, 16]. The characteristics of the temperature modulation needed and its duration are strain specific and depend on the geographical origin of the animal strain [17].

Polyp-to-jellyfish transition can be divided into three successive phases: induction of metamorphosis by temperature shift, strobilation, and jellyfish morphogenesis. Strobilation is a segmentation-like process that starts at the apical part of

⁷These authors contributed equally to this work

⁸Present address: Marine Genomics Unit, Okinawa Institute of Science and Technology, 1919-1 Tancha, Onna-son, Kunigami-gun, Okinawa 904-0495, Japan

*Correspondence: konstantin.khalturin@oist.jp



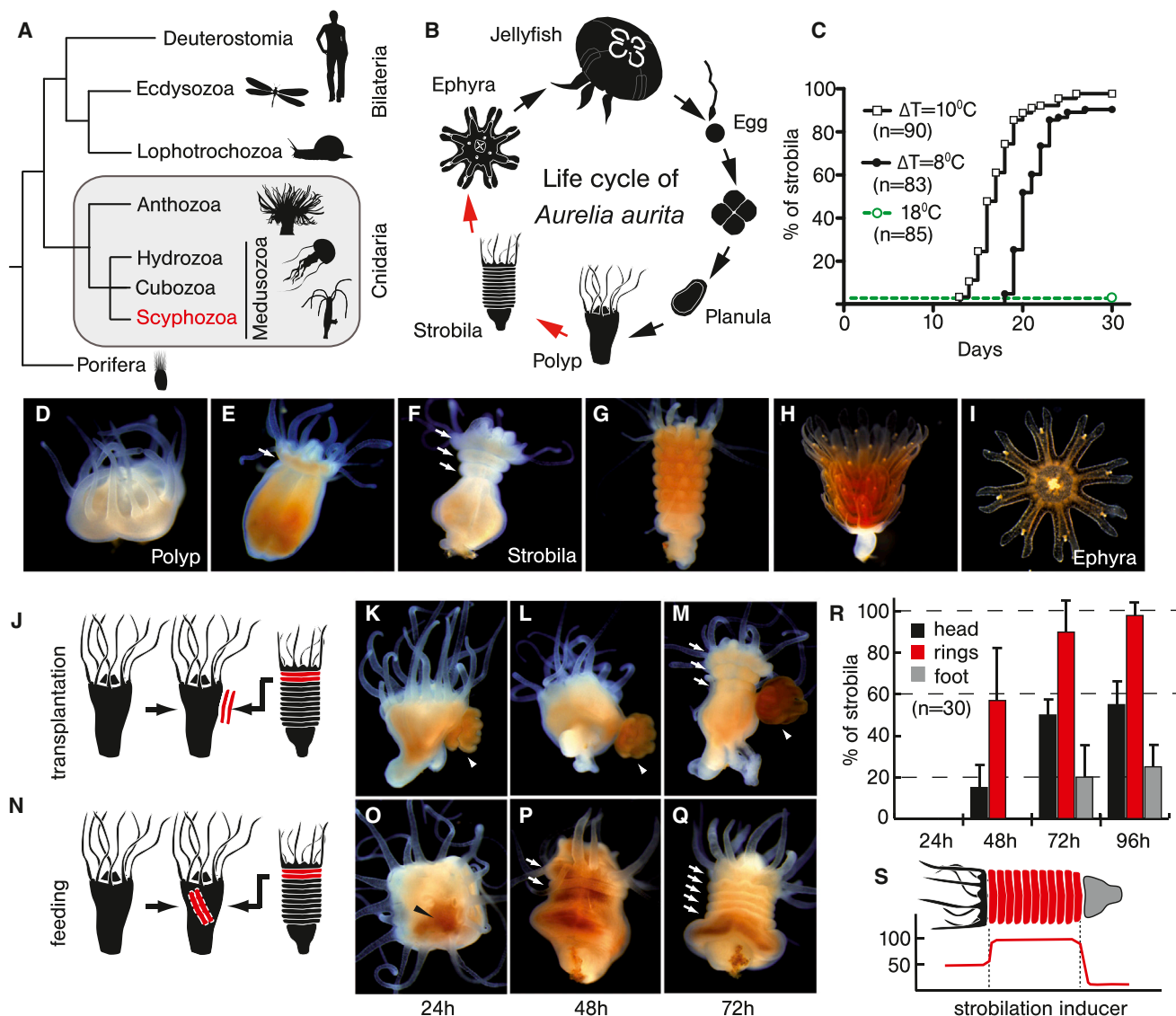


Figure 1. Metamorphosis in *Aurelia aurita* Is Initiated by Temperature Shift and Is Regulated by a Secreted Strobilation Inducer

(A) Scyphozoan jellyfishes belong to the phylum Cnidaria, which is a sister group to all bilaterian animals.

(B) Life cycle of *Aurelia aurita*. Each polyp transforms into multiple ephyra during strobilation.

(C) Polyp-to-jellyfish transition is induced by cold temperature. Polyps maintained at constant temperature ($+18^\circ\text{C}$) do not strobilate. ΔT , temperature shift; open square, cooling from $+20^\circ\text{C}$ to $+10^\circ\text{C}$; closed circles, cooling from $+18^\circ\text{C}$ to 10°C ; n, total number of animals in three independent experiments.

(D–I) Strobilation in *Aurelia*. The polyp (D) is divided into multiple segments (E–G) that develop into young jellyfishes (H and I). White arrows, strobila segments.

(J–M) Metamorphosis induction by transplantation (J). Segmentation starts 72 hr after transplantation (K–M). White arrowheads, transplanted strobila segments; white arrows, newly developed segments.

(N–Q) Metamorphosis induction by feeding with strobila segments (N). Polyp fed with strobila segments 24 hr (O), 48 hr (P), and 72 hr (Q) after feeding. Black arrowhead, strobila segments inside of the polyp; white arrows, strobila segments.

(R) Feeding experiments. The segmented part of the strobila (rings) contains the highest amount of the strobilation inducer.

(S) Putative distribution of the strobilation inducer along the body of the strobila.

See also Figure S1.

the polyp and progresses downward (Figures 1D–1F). As a result, a stack of disk-shaped segments is generated (Figures 1E–1G). Each of those segments subsequently turns into a young jellyfish called an ephyra (Figures 1H and 1I). The young ephyra detaches from the strobila (Figures 1H and 1I), starts independent planktonic life, and within several weeks develops into an adult jellyfish (Figure 1B).

By using a combination of classical transplantation experiments, transcriptomic analysis, and a loss-of-function

approach, we uncovered the molecules critical in controlling the polyp-to-jellyfish transition in the life cycle of *Aurelia*.

Results

Diffusible Molecules Induce Metamorphosis and Strobila Formation

In *Aurelia aurita* (strain Roscoff), polyp-to-jellyfish transition can be induced by temperature shift from $+18^\circ\text{C}$ to $+10^\circ\text{C}$.

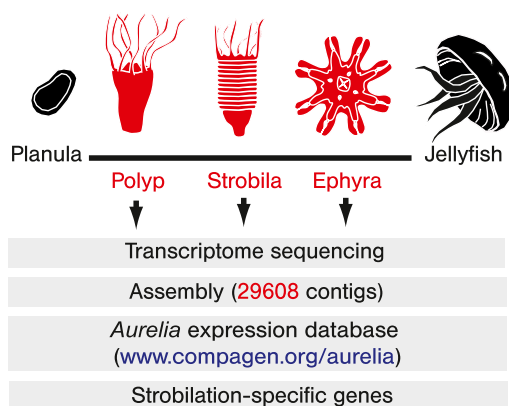


Figure 2. Identification of the Stage-Specific Genes and the Regulators of Metamorphosis

Strobilation-specific genes were identified by comparison of the transcriptomes of polyp, strobila, and ephyra stages. Transcriptomic data are available at NCBI SRA under the accession number SRX019580. See also Figure S2.

After 3 weeks of incubation at +10°C, about 25% of polyps (Figure 1C) show the first morphological sign of metamorphosis—tissue constriction below the head (Figure 1E). Temperature shift is the only necessary manipulation to induce metamorphosis in *Aurelia*.

The wave-like nature of strobilation (Figures 1E–1G) implies the presence of a signaling factor or factors that should initiate and regulate the metamorphosis process. In order to verify this assumption, we performed the transplantation experiments shown in Figure 1J and Figure S1A (available online). Indeed, strobila segments, when transplanted onto noninduced polyps, induce strobilation within 72 hr (Figures 1K–1M). Interestingly, the strobilation process in the recipient polyps starts and progresses from the most apical part of the body and not from the site of transplantation. When strobila segments are fed to noninduced polyps (Figure 1N), the first signs of strobilation are observed even earlier, within 48 hr after feeding (Figures 1O–1Q). Against the expectation, strobila segments are not digested by the polyp and are retained intact in the gastric cavity for several days. Tissues of noninduced polyps or ephyra do not induce strobilation (Figures S1B–S1J). Feeding experiments demonstrate that a different amount of the metamorphosis inducer is present in the head, segments, and foot part of the strobila. As shown in Figure 1R, strobila segments have the strongest inductive capacity, head tissue is less potent, and the least amount of inducer is present in the foot. Curiously, the induction of strobilation by transplantation or feeding is successful only when polyps and strobila belong to the same *Aurelia* strain. Feeding polyps belonging to Baltic Sea or White Sea strains with genetically different strobila of the Roscoff strain does not cause strobilation (Figures S1K–S1M). Taken together, our data indicate that the strobila stage produces diffusible signaling factor(s) capable of inducing metamorphosis. This inductive substance is predominantly located in the segmented part of the strobila (Figure 1S) and is not present in polyp and ephyra stages.

Uncovering Genes and Signaling Cascades Involved in Strobilation

To identify the nature of the strobilation inducer and the molecular machinery of metamorphosis, we sequenced and

compared transcriptomes of the polyp, strobila, and ephyra stages in *Aurelia aurita* (Figure 2). Sequences were de novo assembled (see the Supplemental Experimental Procedures) and integrated into an online database (see *Aurelia Project* at <http://www.compagen.org/aurelia>), and the genes that were preferentially expressed during strobilation were identified (Figure S2A). Detailed analysis of selected genes by in situ hybridization confirmed that the sequencing approach correctly reflects expression profiles (Figures S2B–S2V). One of the findings that attracted our special attention was the identification of the *RxR* gene, which is up-regulated during strobilation. Taking into consideration that retinoic acid (RA) signaling is important for the developmental processes in bilateria and that nuclear hormone receptors including *RxR* are known to be involved in metamorphosis, we investigated the function of RA signaling in more detail.

Retinoic Acid Signaling and Strobilation

The *Aurelia* transcriptome encodes differentially regulated retinol dehydrogenases (RDHs) and a bona fide homolog of the bilaterian *RxR* (Figure S3A and Document S2). *RDH1* is gradually downregulated during strobilation, while *RxR* and *RDH2* are strongly upregulated (Figures 3A and S3B–S3J). Importantly, in the polyps fed with strobila segments, expression of *RxR* receptor is rapidly upregulated prior to the appearance of any morphological signs of strobilation (Figure 3B). Thus, there is a correlation between differential regulation of RA cascade genes and the strobilation process in *Aurelia*.

RDHs and *RxR* receptor are members of the retinoic acid signaling cascade (Figure 3C). RDHs convert retinol (vitamin A) into retinaldehyde, an intermediate in the synthesis of 9-*cis* RA, which in turn activates *RxR* nuclear receptor. Upregulation of *RxR* and *RDH2* led us to hypothesize that retinoic signaling might be involved in the initiation of *Aurelia* metamorphosis in response to temperature shift. In order to test this hypothesis, we performed chemical interference experiments by incubating polyps in retinol, 9-*cis* RA, and the RA cascade inhibitors 4-diethylaminobenzaldehyde (DEAB) and UVI3003. DEAB blocks the aldehyde dehydrogenases necessary for the production of 9-*cis* RA from retinaldehyde, and UVI3003 is a highly specific antagonist that prevents *RxR* activation (Figure 3C).

Incubation of *Aurelia* polyps at +18°C in artificial sea water (ASW) containing 1 μM retinol or 1 μM 9-*cis* RA induced strobilation after 7 and 12, days respectively (Figure 3D). Therefore, retinol and 9-*cis* RA are able to directly induce strobilation, bypassing the temperature-sensing step. Retinol and 9-*cis* RA induce strobilation approximately two times quicker than the temperature shift from +18°C to +10°C (7–12 versus 19–21 days; Figure 1C), but about two times slower than transplantation or feeding of strobila rings (3 or 2 days; see Figures 1J–1Q). Strobilation induction by retinol or 9-*cis* RA is significantly delayed in the presence of *RxR* antagonist (1 μM UVI3003; Figure 3D). In coinubation experiments (Figure 3D; retinol + UVI3003 or 9-*cis* RA + UVI3003), polyps kept at +18°C start to strobilate only after 17 days. As expected for the inhibitor, which blocks the activity of enzymes producing 9-*cis* RA from retinaldehyde, DEAB slows down strobilation in animals incubated in retinol (Figure S3K), but does not influence strobilation in polyps incubated in 9-*cis* RA (Figure S3L). Surprisingly, 10 μM DEAB does not inhibit normal temperature-induced strobilation at +10°C (Figure S3M),

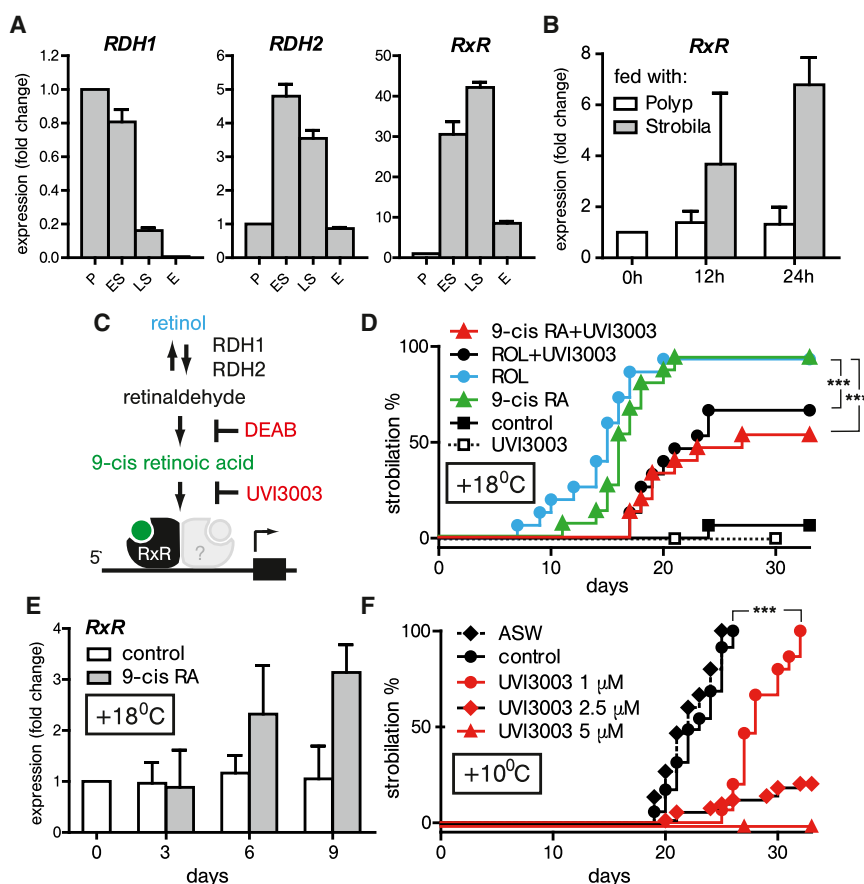


Figure 3. Retinoic Acid Signaling Is Necessary for the Metamorphosis in *Aurelia*

(A) Expression of retinoic X receptor (*RxR*), retinol dehydrogenase 1 (*RDH1*), and retinol dehydrogenase 2 (*RDH2*) during strobilation. P, noninduced polyp; ES, early strobila with one segment; LS, late strobila with several segments; E, ephyra. (B) *RxR* upregulation in feeding experiments. Expression levels in nonfed animals (0 hr) and after feeding with strobila and polyp tissue (12 hr and 24 hr) are shown. (C) Schematic representation of retinoic acid signaling cascade. (D) Strobilation induction by 1 μ M solution of retinol (ROL) or 9-*cis* RA at +18°C. Coincubation of polyps in ROL or RA and 1 μ M UVI3003 slows down strobilation induction. The total number of animals in each treatment is $n = 30$. *** $p < 0.0001$, log-rank (Mantel-Cox) test. (E) *RxR* expression in polyps incubated in 9-*cis* RA (1 μ M) at +18°C. Expression in nontreated animals (0) and after 3, 6, and 9 days of incubation is shown. (F) Temperature-induced strobilation at +10°C is repressed by UVI3003 (1 μ M, 2.5 μ M, and 5 μ M). The total number of animals in each treatment is $n = 30$. *** $p < 0.0001$, log-rank (Mantel-Cox) test. Expression levels in (A), (B), and (E) were determined by quantitative RT-PCR. *EF1 α* was used for equilibration. Mean expression \pm SD is shown ($n = 3$). See also Figure S3 and Table S1.

which is unexpected and implies that additional strobilation regulators might be present.

As shown on Figure 3E, incubation of polyps in 1 μ M 9-*cis* RA causes upregulation of *RxR* similar to that in the feeding experiments (Figure 3B) or during the temperature induction (Figure 3A). After 6 days of incubation, the first changes in *RxR* expression level are detectable, and after 9 days of incubation, its expression is upregulated 3-fold. Importance of the *RxR* for the metamorphosis is additionally substantiated by the fact that the temperature-induced strobilation can be inhibited by UVI3003 in a concentration-dependent manner (Figure 3F). As shown in Figure 3F, strobilation is significantly delayed in 1 μ M solution of UVI3003, and it is completely repressed in 5 μ M solution.

Thus, *RxR* receptor seems to be important for the strobilation process, and 9-*cis* RA might serve as a signaling molecule in *Aurelia*. We have not directly shown that 9-*cis* RA is produced in this species, but the upregulation of *aRDH2* and the retardation of strobilation by DEAB both speak in favor of this possibility. Incubation in retinol or 9-*cis* RA can functionally substitute the temperature shift that induces strobilation under natural conditions. Hence, retinoic acid signaling might serve as a link between yet unknown temperature-sensing receptor and the downstream genes responsible for the onset of metamorphosis. It is also important to mention that 9-*cis* RA and retinol, even in their highest nontoxic concentrations (5 μ M), are not able to induce strobilation within 48 hr as it happens when polyps are fed with strobila segments. This indicates that 9-*cis* RA is important, but not the only regulator of strobilation.

Unbiased Identification of Strobilation-Inducing Molecules

In the *Aurelia* transcriptome, we identified 345 strobila-specific genes (Figure S2A). Based on the fact that only strobila tissue induces metamorphosis in transplantation and feeding experiments (Figures 1J–1Q and S1A–S1J), the gene that encodes the strobilation inducer must be strobili specific. In order to narrow down the list of potential candidates, we used microarray to analyze the changes in the *Aurelia* transcriptome during the temperature-induced strobilation. Our goal was to identify genes that are not expressed in the polyp stage, are upregulated in response to cold temperature, reach their highest expression level in the strobila stage, and are downregulated again in ephyra. Additionally, we made use of the observation that *de novo* methyltransferase 1 (*DNMT1*) is strongly upregulated during strobilation and that 5-aza-cytidin, an inhibitor of DNA methylation by DNMT1, retards the onset of strobilation (Figures S4A and S4B). We assumed that the expression level of the inducer should be lower in 5-aza-cytidin-treated polyps than in the corresponding DMSO controls. Expression profiles were determined in induced polyps (24 hr, 14 days, and 16 days in DMSO or 5-aza-cytidin at +10°C), early strobila (one segment), late strobila (five segments), and freshly detached ephyra (Figure 4A, http://www.compagen.org/aurelia/aaurlatlas_ma.html, and EBI Array Express E-MTAB-1960).

In total, 27 contigs exhibit the expression dynamics predicted for the strobilation inducer. Groups of contigs with identical expression dynamics represent splice variants or 5'/3' untranslated regions of the same gene (for example, clusters 26669, 26813, 26229, 15345, 1285, 390 and 4884, 631, 913). Three genes (*CL390*, *CL112*, and *CL631*) attracted our special

attention due to their drastic upregulation at +10°C. As shown in Figure 4B, the increase in the amount of transcript between polyp and early strobila is more than 35,000-fold for *CL390*, 2,700-fold for *CL112*, and 3,200-fold for *CL631*.

Transcript localization of *CL390*, *CL112*, and *CL631* was examined by in situ hybridization in noninduced polyps, in induced polyps with the first constriction (VES), in early strobila (ES), in late strobila (LS), during ephyra morphogenesis, and in ephyra. As shown in Figures 4C–4Q, the candidate genes are not expressed in the polyp, but all of them are strongly upregulated during strobilation.

All three candidate genes encode proteins lacking similarity to any known proteins from other animals (BLASTP *e* value < 1×10^{-5}). Thus, they most probably represent Scyphozoa-specific or even *Aurelia*-specific genes. All three proteins contain a putative signal peptide sequence at the N terminus (Figure 4R). *CL390* protein consists of two qualitatively different regions: an N-terminal portion containing large numbers of hydrophobic amino acids and a C-terminal portion containing highly charged motifs made of arginine-rich repeats (Figure 4S). *CL112* contains a domain consisting of six cysteine residues with low sequence similarity to epidermal growth factor (EGF; *E* = 1×10^{-2}). Similar to *CL390*, *CL631* contains large proportions of hydrophobic amino acids in its N-terminal region. Three repeats in the C-terminal region of *CL631* are separated by the putative endopeptidase processing sites KR and KK.

CL390, *CL112*, and *CL631* encode novel secreted proteins, and due to their strong expression during metamorphosis, they might be considered as potential strobilation inducers. *CL390*, however, seems to be the most promising candidate since it is not expressed at the polyp stage, it is strongly upregulated in strobila in response to the temperature changes, and its expression is drastically downregulated in the ephyra stage.

Identification of a Temperature Dependent “Timer” for the Onset of Metamorphosis

In nature, polyps start to strobilate in spring after being exposed to a prolonged period of cold water temperature. How does the metamorphosis-controlling system distinguish winter from occasional short-term temperature fluctuations? Theoretically, there must be a minimal duration of the “cold” period that causes metamorphosis, and such a system would require cold-sensitive genes to operate.

Indeed, *CL390*, *CL112*, and *CL631* are cold sensitive and an increase in their transcript levels occurs earlier than the onset of segmentation (Figure 5A). The most intriguing dynamics can be observed with *CL390*. While the upregulation of *CL112* and *CL631* is detectable only after 17 and 19 days, the upregulation of *CL390* is first detectable already after 9 days at +10°C.

To determine the minimal duration of the cold period needed to induce strobilation, we placed groups of polyps at +10°C and returned them back to +18°C after 6, 9, and 12 days of cold treatment (Figure 5B, inset; Figure S5A). As shown in Figure 5B, none of the polyps incubated at +10°C for just 6 days metamorphosed, while incubation for 9 days was sufficient to induce strobilation. Animals kept at +10°C for 12 days exhibit the same strobilation kinetics as the animals in the control group, which remained at +10°C. Expression of *CL390* in the polyps that were returned back to +18°C after 3, 6, and 9 days of cooling is shown in Figures 5B (inset) and S5A. The expression level of *CL390* shows fluctuations and has a

tendency to decrease at +18°C after the initial upregulation at +10°C.

Detailed analysis of *CL390* expression by real-time PCR (Figure 5C) shows that at +10°C the amount of transcript increases exponentially, with mean upregulation of 5.5× after 6 days, 31× after 9 days, and 110,000× after 19 days. The amount of *CL390* transcript in a polyp is positively and directly correlated with the amount of time spent by *Aurelia* polyps at low temperature. Our results indicate that as soon as the upregulation exceeds the threshold of about 15-fold (between 6 and 9 days at +10°C), the strobilation program is activated and becomes independent from temperature input (Figure 5C). *CL390* therefore represents an example of a novel temperature-dependent “timer” whose expression level allows *Aurelia* polyps to “measure” the duration of a cold period.

As shown in Figure 5A, genes involved in retinoic acid signaling (*RDH1/RDH2* and *RxR*) are also sensitive to temperature changes. The upregulation of *RxR*, similar to that of *CL390*, precedes morphological changes and is detectable after 6 days at +10°C. Interestingly, *CL390* expression can be directly activated by incubation of polyps in 9-*cis* RA at +18°C (Figure 5D). This result indicates a possible link between retinoic acid signaling and the activation of *CL390* in *Aurelia*. In support of this view, the 5′ flanking region and the first intron of *CL390* contain three putative binding sites for *RxR* nuclear hormone receptor (Figures S5B–S5D). We did not perform functional tests for these elements, but the identical half sites with the sequence AGGTCA from the promoters of *crystallin* genes have been shown previously to bind *RxR* of *Tripedalia cystophora* [13]. Taking into consideration the high degree of sequence conservation between DNA binding domains (DBDs) of *RxRs* from *Aurelia* and *Tripedalia* (Figure S5E), the probability of *RxR* binding to AGGTCA elements in the promoter of *CL390* is relatively high.

CL390 Acts as Strobilation Inducer in *Aurelia*

On the cellular level, cooling activates the expression of *CL390* in the ectodermal epithelial cells, which initially form small patches (Figures 5E, 5F, and S5F) that increase in number and expand in size. Several hours before the initiation of the segmentation process, all ectodermal epithelial cells of a polyp (except the ones in the tentacles and in the foot) become *CL390* positive (Figure 5G).

Similar upregulation and spreading of *CL390* expression is observed in transplantation and feeding experiments. As described previously (see Figures 1J–1Q), strobilation can be induced by transplantation or feeding within 72 and 48 hr, respectively. As shown by in situ hybridization in Figure 5H, transplantation of strobila segments induces local upregulation of *CL390* in the region adjacent to the transplant (dotted line in Figure 5H). A patch of *CL390*-expressing cells surrounds the area where the transplant was located (transplanted strobila tissue has been removed from the recipient animal prior to fixation). In the feeding experiments, *CL390* is systemically and strongly upregulated in all ectodermal epithelial cells throughout the polyp body within 24 hr (Figure 5I).

In order to directly examine the influence of *CL390*, *CL112*, and *CL631* on strobilation, we developed RNAi technology for *Aurelia* (see the Supplemental Experimental Procedures). As shown in Figures S5H and S5J, by electroporating early strobila with double-stranded RNA (dsRNA) of *CL390* or *CL112*, we were able to repress the expression of the corresponding genes. Electroporation of control dsRNA (*GFP* or *CL1008*) did not influence gene expression (Figures S5G and

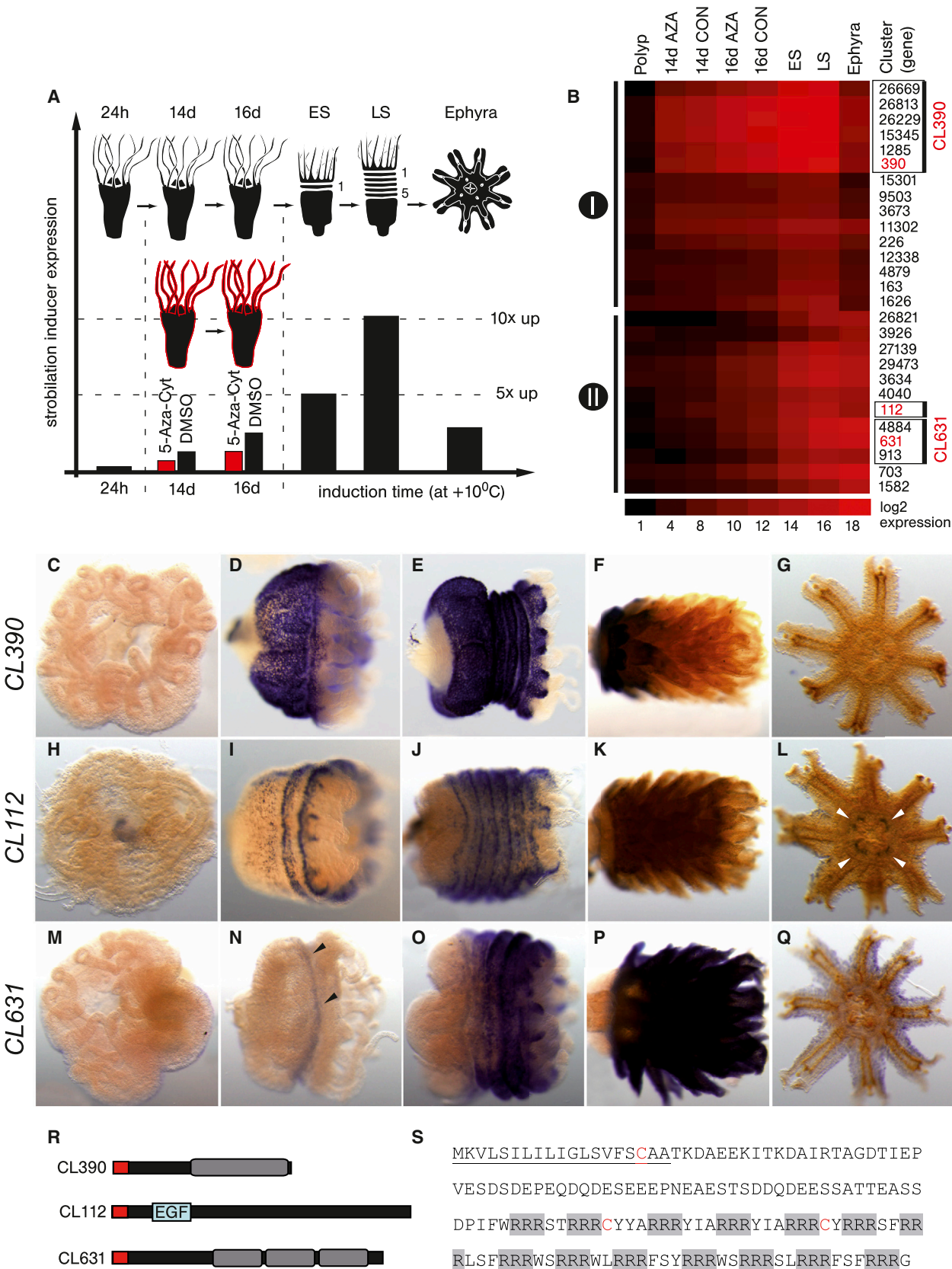


Figure 4. Identification of the Candidate Strobilation Inducers by Microarray Approach

(A) Microarray experiment design. The hypothetical expression profile of the strobilation inducer is shown as a bar diagram along the x axis. 5-Aza-cyt, animals treated with 5-aza-cytidine (5 μ M); DMSO, solvent control; ES, early strobila with one segment; LS, late strobila with five segments.

(legend continued on next page)

S5I). To test the function of genes potentially involved in strobilation, we electroporated induced polyps (after 6 days at +10°C) with dsRNA of *CL1008* (ephyra-specific gene used as a control), *CL390*, *CL112*, and *CL631*. As shown in Figure 5J, we observed no significant difference in strobilation kinetics between animal groups electroporated with *CL1008*, *CL631*, or *CL112*. In contrast, animals electroporated with *CL390* dsRNA strobilated slower than did the control animals (*CL1008*). The inhibition was not complete, which is not surprising when taking into consideration that we have depleted only about 60% of the *CL390* transcript (inset in Figure 5J). Our results, however, indicate that *CL390* is causally involved in strobilation and might represent the strobilation inducer.

CL390-Derived Synthetic Strobilation Inducers

CL390 encodes a secreted protein with an unusual C-terminal part where arginine repeats separate di- and tripeptides with the sequences SF, LSF, WS, WL, FSF, WS, SL, and FSF (Figure 6A). To directly test the function of *CL390* in strobilation, we fed polyps with the full-length recombinant protein fused to GFP (Figures S6A–S6D) and incubated the polyps in synthetic peptides (50 μM) representing subfragments of *CL390* (Figures 6A and S6E). Feeding causes formation of segment-like constriction below the head of *Aurelia* polyps (see Figure S5D), but the segmentation does not progress further. In contrast to that, synthetic peptide with the sequence WSRRLWL induces strobilation within 72 hr of incubation at +18°C (Figure 6B). Other peptides tested do not induce strobilation (Figures 6A and S6E). These results indicate that *CL390* might be the precursor of the strobilation inducer, which becomes biologically active after being processed into smaller fragments. As shown in Figure 6C, according to in silico structure prediction, the C-terminal part of *CL390* forms a helix where aromatic amino acids separated by three arginins are located in close proximity to each other (F127–W131 and Y143–W147). In case of the WSRRLWL peptide, indole rings of two tryptophans are also located in close proximity and in mutually perpendicular planes (Figure S6F). Such a close positioning of the aromatic rings is similar to the core part of the indole derivative indomethacin (Figure 6D), which has been recently shown to induce strobilation in the Japanese strain of *Aurelia aurita* [14]. Indomethacin is an anti-inflammatory drug that functions via inhibition of cyclooxygenases (COX1/COX2). The transcriptome of *Aurelia aurita* and the genomes of *Nematostella*, *Hydra*, and *Acropora* do not contain homologs of COX-1 and COX-2. Thus, in light of the observations described above, the inductive activity of indomethacin might be explained by its structural similarity to the naturally occurring strobilation hormone of *Aurelia* encoded by *CL390*.

In order to identify the minimal pharmacophore able to activate strobilation, we screened indole and tryptophan derivatives and identified four substances with a strong capacity to induce strobilation at 50 μM (see Figure S6G and Table S2

for the complete list of the compounds tested). As shown on Figure 6D, all active compounds share a core structure made of an indole ring and methyl or carboxylic groups at position two. Despite the structural similarity, compounds (1)–(5) have drastically different inductive capacities in the Roscoff strain of *Aurelia* (Figure 6E). Indomethacin (1) induces strobilation only after 6 days of incubation, while 5-methoxy-2-methylindole acetic acid (2) and 5-methoxyindole-2-carboxylic acid (3) do so after 4–5 days, 2-methylindole (4) after 3 days, and 5-methoxy-2-methylindole (5) within 48 hr. Interestingly, at a concentration of 50 μM, 5-methoxy-2-methylindole induces strobilation with the same kinetics as feeding with strobila segments. The inductive capacity of 5-methoxy-2-methylindole remains identical within a concentration range between 50 μM and 5 nM (Figure 6F). Even at a concentration of 1 nM, strobilation is induced after 48 hr and all of the incubated polyps start to metamorphose within 8 days. Only at a concentration of 0.1 nM is the inductive effect considerably reduced, and it is completely absent at a concentration of 0.01 nM.

Thus, the *CL390* gene appears to encode the precursor of the strobilation hormone in *Aurelia aurita* and 5-methoxy-2-methylindole appears to represent its minimal pharmacophore.

Discussion

Molecular Toolkit of Strobilation in *Aurelia*

Alternation between larval and adult stages with drastic morphological, physiological, and behavioral differences is a fundamental metazoan feature [3]. Life cycles with various levels of complexity are present in all animal phyla, but the molecular machinery driving the transitions between life stages has been deciphered in just a few model organisms [1–3, 11].

In amphibians and arthropods, where the molecular basis of metamorphosis is characterized in detail, the activation of metamorphosis has always two successive steps—a neuronal one and an endocrine one. In both animal groups, the core module of life-cycle regulation consists of two nuclear hormone receptors that cooperatively control the activation of the downstream metamorphosis genes (Figure 7A).

In amphibians, thyroid-stimulating hormone (TSH) from the pituitary gland regulates the production of thyroid hormone (TH), which induces tadpole transformation into juvenile frog [18, 19]. Thyroid hormone is a condensation product of two iodinated tyrosins derived from a high-molecular-weight protein precursor. The cascade of downstream genes leading to metamorphosis is activated by a heterodimer of thyroid hormone receptor (TR) and RXR. TR homologs are present in Chordata, Urochordata, Cephalochordata, and Hemichordata [3]. In the protostomian lineage, TRs have been identified in the plathelminths *Schistosoma mansoni*, *S. japonicum*, and *Schmidtea mediterranea*, as well as in the mollusk *Lottia gigantea* and the arthropod *Daphnia pulex* [20]. TR genes

(B) Clusters with the expression profile predicted for the strobilation inducer. Clusters representing the splice variants of the same gene are boxed. Numbers, cluster identifiers; ES, early strobila; LS, late strobila; I, clusters where expression is strongly downregulated in ephyra; II, clusters without strong downregulation in ephyra. The heatmap represents *EF1α* normalized expression values after log₂ transformation.

(C–G) *CL390* is strongly upregulated during strobilation and is not expressed in ephyra.

(H–L) *CL112* is expressed in a subpopulation of endodermal cells during strobilation and in the manubrium of ephyra.

(M–Q) *CL631* is exclusively expressed in the segments of strobila and in ephyra. Black arrowhead, segment border.

(R) Protein domain organization of *CL390*, *CL112*, and *CL631*. Putative signal peptide sequence is shown in red; gray boxes, internal repeats; light-blue box, EGF-like domain (see also Figures S4C and S4D).

(S) *CL390* protein. Arginine repeats are highlighted in gray. Cystein residues are shown in red. Putative signal peptide sequence is underlined.

Polyp stage (C, H, M); early strobila (D, I, N); late strobila (E, J, O), late strobila undergoing ephyra morphogenesis (F, K, P), and ephyra (G, L, Q) are shown. See also Figure S4.

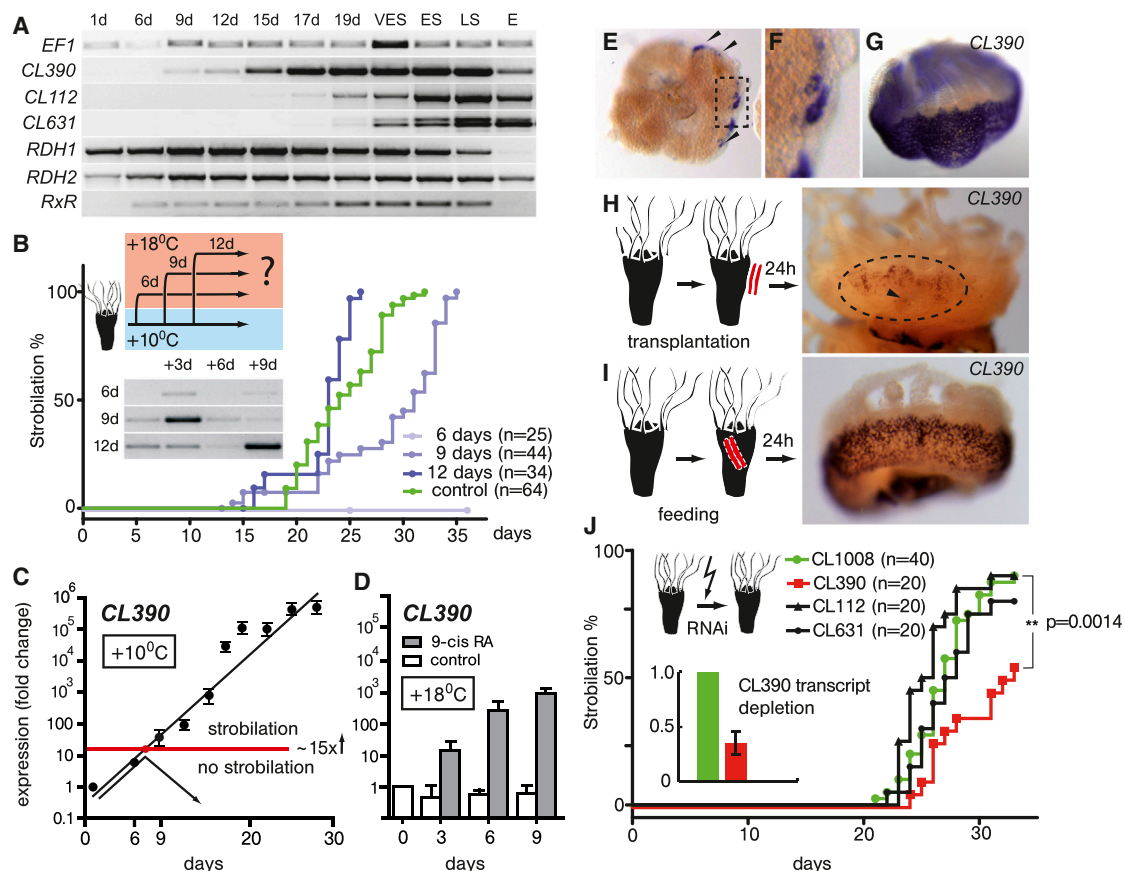


Figure 5. Functional Analysis of the *CL390* Gene

(A) Induction of strobilation at $+10^{\circ}\text{C}$. 1d, noninduced polyp; 6d–19d, expression in polyps incubated for 6–19 days; VES, very early strobila with one constriction; ES, early strobila; LS, late strobila; E, ephyra; *EF1*, elongation factor 1- α ; *RDH1/2*, retinol dehydrogenase 1/2; *RxR*, retinoic X receptor. Lanes were cropped from the original image shown in Figure S5A.

(B) Minimal duration required for the temperature induction. Strobilation curves and *CL390* expression levels after 3, 6, and 9 days (+3d, +6d, and +9d in the insert) are shown. Control, polyps continuously incubated at $+10^{\circ}\text{C}$.

(C) *CL390* expression is exponentially increased at $+10^{\circ}\text{C}$. Horizontal red line, threshold level for strobilation.

(D) *CL390* expression in polyps treated with 9-*cis* RA (1 μM) at $+18^{\circ}\text{C}$. Expression in nontreated animals (0) and after 3, 6, and 9 days of incubation.

(E–G) Expression of *CL390* before the onset of segmentation (E). A close-up view of the area boxed in (E) is shown in (F). *CL390* expression several hours before the appearance of the first constriction is presented in (G). Black arrowheads, groups of *CL390*-positive cells.

(H) Local upregulation of *CL390* in transplantation experiment. Dotted line, area of the tissue contact between the recipient polyp and the transplant; arrowhead, position of the transplant.

(I) Systemic upregulation of *CL390* after feeding with strobila segments.

(J) Influence of *CL390*, *CL112*, and *CL631* knockdown on the temperature-induced strobilation. dsRNA of *CL1008* (ephyra-specific gene) was electroporated as a control. Expression of *CL390* is downregulated for about 60% (quantitative RT-PCR data \pm SD in the insert). N, total number of electroporated polyps in three experiments. Strobilation curves compared by log-rank (Mantel-Cox) test ($p = 0.0014$).

Expression levels in (C) and (D) were determined by quantitative RT-PCR. Mean expression \pm SD ($n = 3$). *EF1 α* was used for equilibration. See also Figure S5.

have been lost in insects and nematodes [3] and have not been identified in cnidarians.

In insects, the major inducers of metamorphosis are prothoracicotropic hormone (PTTH) and ecdysone (see Figure 7A). PTTH is a neuropeptide that activates ecdysone production in the prothoracic gland. The sequence of PTTH considerably differs in *Manduca*, *Drosophila*, and *Bombyx mori* [1], and it has not been identified outside insects. In contrast to PTTH, ecdysone has a broader phylogenetic distribution, and its derivatives serve as hormones throughout the arthropods [21]. In insects, similar to that in amphibians, the target genes responsible for the metamorphosis are also activated by a heterodimer that in this case consists of Ultraspiracles (homologous to *RxR*) and the ecdysone nuclear receptor (*EcR*).

In *Aurelia*, we show that *RxR* transcription factor is involved in the polyp-to-jellyfish transition and that a secreted *Aurelia*-

specific protein (*CL390*) is the best candidate for the precursor of the strobilation hormone (Figure 7A). In the polyps incubated in 9-*cis* RA, the *RxR* and *CL390* genes are upregulated, indicating an interaction between *RxR* and *CL390*. Thus, it is reasonable to propose that in *Aurelia*, similar to that in insects and amphibians, the *RxR* receptor belongs to the core molecular module that regulates the polyp-to-jellyfish transition. There is also an additional striking analogy. Thyroid hormone in vertebrates is a condensation product of an aromatic amino acid tyrosine. In *Aurelia*, the minimal pharmacophore of the strobilation hormone is based on an indole ring structure that is nothing else but the core element of another aromatic amino acid, tryptophan. Our data therefore suggest that the polyp-to-jellyfish transition in *Aurelia* follows at least some of the general principles of metamorphosis regulation known from more advanced animals.

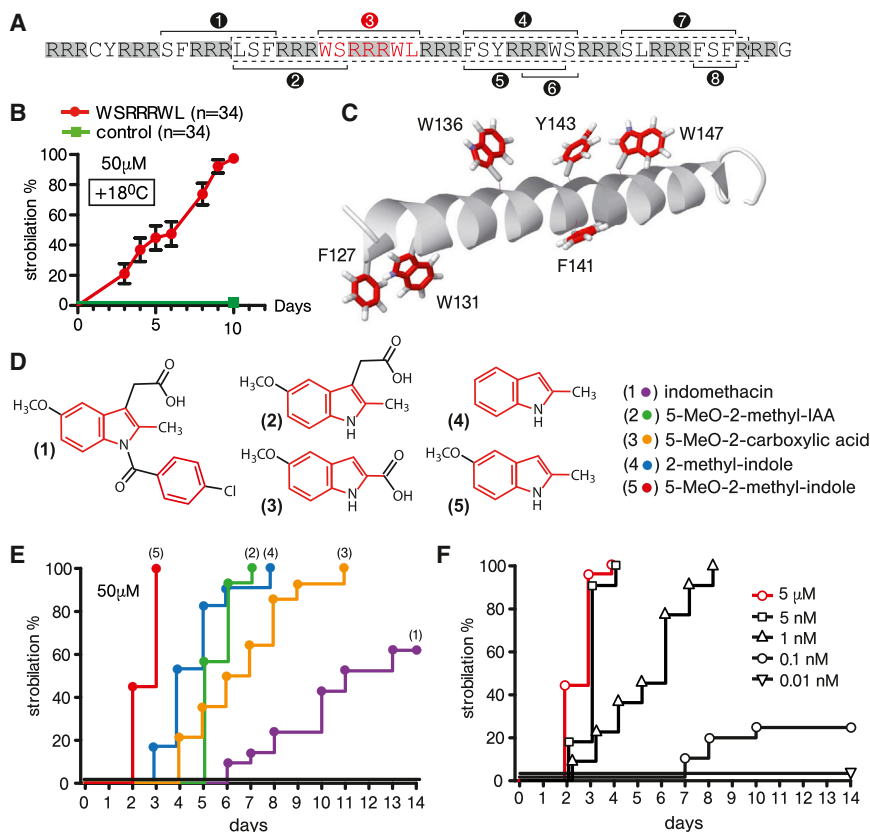


Figure 6. Synthetic Activators of Strobilation

(A) C-terminal part of CL390 protein. Synthetic peptides are shown by brackets (1–8). The active fragment is highlighted in red. The fragment used for in silico structure prediction is boxed with a dotted line.

(B) Strobilation induction by WSRRRWL peptide. Control, DMSO incubation. Mean of four independent experiments \pm SE is shown; n, total number of polyps incubated.

(C) Predicted structure of the C-terminal part of CL390. Aromatic rings are highlighted in red.

(D) Chemical induces of strobilation. Aromatic rings are highlighted in red.

(E) Strobilation curves in 50 μ M solution of indomethacin (1), 5-methoxy-2-methyl indole acetic acid (2), 5-methoxy-2-carboxylic acid (3), 2-methyl indole (4), and 5-methoxy-2-methyl indole (5).

(F) Strobilation curves at different concentrations of 5-methoxy-2-methyl indole.

See also Figure S6 and Table S2.

A Temperature Dependent Molecular Timer for the Onset of Metamorphosis

Strobilation in *Aurelia* polyps is induced by an environmental signal: lowering of the water temperature. This probably insures that strobilation and successive jellyfish development take place in the environmentally favorable conditions of spring and summer after the period of low water temperature during the winter season. Strobilation induction by temperature shift phenomenologically resembles the vernalization process in plants, where a cold winter period is necessary to allow flowering [22]. In plants, there is a minimal duration period required for vernalization, and this minimal permissive duration of cold temperature is strain specific [23]. A similar logic seems to be in place for the strobilation induction in *Aurelia*, which uses cold temperature as a trigger.

Temperature perception per se has a limited value for making a decision whether to strobilate or not. An essential component is a “memory unit” or “timer,” which has to record the duration of the low-temperature period. In order to monitor seasonal changes, polyps must be able to distinguish between short-time temperature fluctuations and a season-related temperature decrease in the winter period.

We have shown that at low temperatures, the amount of CL390 transcript steadily increases with time and that at high temperatures the transcript level drops. Thus, the level of CL390 activation serves as information about the duration of the cold exposure. Such an expression behavior indicates that CL390 plays a role of a temperature-dependent “timer” that measures the duration of the winter period and initiates the metamorphosis program if the activation threshold has been reached.

Phylogenetic Distribution of RxRs and the Presence of a Jellyfish Stage in the Life Cycle

The RxR receptor has an intriguing phylogenetic distribution among cnidarians. Genomes of two anthozoan species sequenced so far [24, 25], as well as the genome of *Hydra* [26], contain no bona fide RxR receptors.

None of these animals have a jellyfish stage in their life cycle. To the contrary, *Tripedalia*, *Aurelia*, and *Clytia* all have a jellyfish stage and also possess RxR receptors (Figures 7B and S3A). Is that a pure coincidence?

In *Aurelia*, the RxR is strongly upregulated during strobilation and is downregulated in the ephyra stage. Incubation with 9-*cis* RA and retinol can induce strobilation, while the RxR antagonist UVI3003 represses it. It has been shown previously that the RxR receptor of *Tripedalia* (jRxR) has a strong affinity to 9-*cis* RA and can bind as monomer to the promoters of *J1A* and *J1B* crystallins [13]. In this cubozoan species, RxR protein is highly abundant in small polyps and in polyps undergoing metamorphosis and disappears sharply (<1 day) after the young ephyra are released [13]. Results in *Tripedalia*, therefore, fit well to our observations in *Aurelia* and suggest that the retinoid signaling might be important for the development of a jellyfish stage.

Retinoic acid signaling has multiple roles in bilaterian development, and the same can be true for Cnidaria. By using exogenous retinoids and pharmacological RxR antagonist, we cannot exclude the possibility that RA metabolism has function in a separate aspect of ephyra formation, whose ectopic activation may indirectly promote strobilation in *Aurelia*. Thus, it will be interesting to further check the correlation between the presence of RxR receptor, activity of retinoic acid signaling, and the development of a jellyfish stage in the broader range of cnidarian species.

Conclusions

Our results underscore the importance of Scyphozoa for evolutionary studies and indicate that nuclear hormone receptors are core elements in the life-cycle regulation machinery

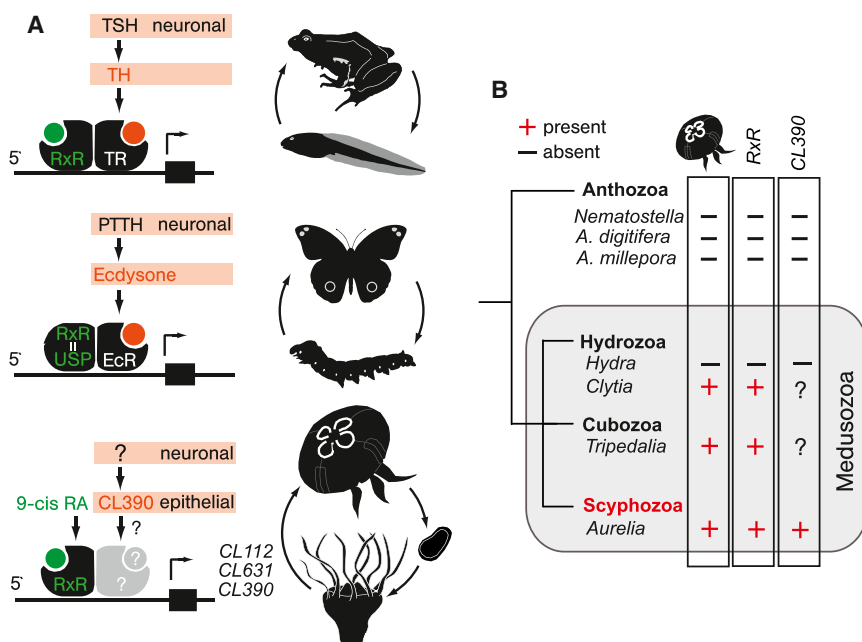


Figure 7. Molecular Machinery of Metamorphosis in *Aurelia*—Comparative Aspects

(A) Core regulators and signaling molecules that are important for metamorphosis in amphibians, insects, and *Aurelia*. TSH, thyroid-stimulating hormone; TH, thyroid hormone; PHHT, prothoracicotropic hormone; 9-*cis* RA, 9-*cis* retinoic acid; TR, thyroid hormone receptor; EcR, ecdysone receptor; RxR, retinoic X receptor; USP, ultraspiracles. CL112, CL631, and CL390 indicate *Aurelia* genes highly upregulated during metamorphosis.

(B) Phylogenetic distribution of the retinoic X receptor in Cnidaria. RxR nuclear hormone receptor is present in scyphozoa (*Aurelia*), cubozoa (*Tripedalia*), and Hydrozoa (*Clytia*), which all possess a jellyfish stage in their life cycle. RxR receptor is absent in the sequenced genomes of Anthozoa and *Hydra*.

throughout the animal kingdom. Identification of the strobilation inducer of *Aurelia* and its minimal pharmacophore also has a potential practical application. In the future, this knowledge may lead to the development of powerful strobilation antagonists that can be used to control jellyfish blooms.

Experimental Procedures

Aurelia aurita Strains and Culturing Conditions

Experiments were carried out using *Aurelia aurita* strains Roscoff, Baltic Sea, and White Sea. Animals were cultured in ASW (Reef Crystals) at 18°C or 20°C. Polyps were fed twice per week with freshly hatched *Artemia* nauplii. Strobilation in the Roscoff strain was induced by incubation of polyps at 10°C.

Transcriptome Sequencing and Assembly

mRNA was isolated from whole animals using the Illustra QuickPrep Micro mRNA Purification Kit (GE Healthcare). Double-stranded cDNA libraries were constructed using the SMART PCR cDNA Synthesis Kit (Clontech). Libraries were sequenced using GS FLX sequencer (Roche). Raw reads have been deposited at the Sequence Read Archive (SRA) of NCBI under the project accession number SRA012593. Final transcriptome assembly (db454_aurelia_celera_v02) is available at <http://www.compagen.org/aurelia/datasets.html>.

Microscopic Analysis

Images were taken on Axioscope fluorescence microscope with Axiocam digital camera (Zeiss) and on SZX16 stereomicroscope with DP71 camera (Olympus).

Chemical Interference Experiments

Stock solutions of 9-*cis* RA (1 mM), retinol (1 mM), UVI3003 (2 mM), and DEAB (20 mM) were prepared in ethanol and stored at −70°C. Single polyps were incubated in 1 ml ASW containing 9-*cis* RA or retinol in 48-well plates. DEAB was added in the final concentration of 10 μM. Control animals were incubated in 1 ml ASW with 0.15% ethanol and nontreatment groups in ASW. Polyps were incubated in the dark at 18°C or 10°C.

Synthetic peptides were ordered from Eurogentec (see Figure S6E). Stock solutions (25 mM) in DMSO were stored as 2 μl aliquots at −70°C. Polyps were incubated in 1 ml ASW containing 50 μM peptide in 48-well plates (2 μl peptide per 1 ml ASW) at 18°C. DMSO solution in ASW (0.2%) was used as a control. Indole derivatives were ordered from Sigma (see

dissolved in DMSO. Solvents (EtOH or DMSO) in the corresponding dilution were used in controls. Solutions were exchanged every day.

In Situ Hybridization

Animals for in situ hybridization were relaxed in ice-cold 2% urethane (in ASW) and fixed overnight with freshly prepared 4% paraformaldehyde (in ASW) at +4°C. Probes were labeled with DIG-UTP and detected by AP-conjugated anti-DIG antibody and NBT-BCIP solution (Roche). See the step-by-step protocol in the [Supplemental Experimental Procedures](#).

Microarray Experiments

Microarray for *Aurelia aurita* strain Roscoff has been designed using Agilent eArray software. Raw microarray image files were processed by Feature Extraction 10.7 Image Analysis software (Agilent). Mean gProcessedSignal values across all the samples were normalized using *elongation factor 1 alpha* (EF1a) expression. Normalized expression values are available online (http://www.compagen.org/aurelia/aaurl_atlas_ma.html) and in the form of the SQL database (http://www.compagen.org/aurelia/aaurl_sql.php). The user manual for microarray data access and retrieval is available at <http://www.compagen.org/aurelia/help.html>.

RNAi

Expression of CL112, CL390, and CL112 was downregulated by electroporation with dsRNA (see the detailed protocol in the [Supplemental Experimental Procedures](#)).

Accession Numbers

The GenBank accession numbers for the sequences reported in this paper are as follows: EF1α (KC341734), RXR (KC341729), RDH1 (KC341731), RDH2 (KC341733), DNMT1 (KC341725), CL390 (KC341732), CL112 (KC341723), CL631 (KC341722), CL1008 (KC357675), 16S_Roscoff (KC767898), 16S_Baltic (KC767897), 16S_White_sea (KC767899), ITS1_Roscoff (KC767900), ITS1_Baltic (KC767902), ITS1_White_sea (KC767901), and RxR of *Clytia* (KC767903). Transcriptomic data were deposited to NCBI SRA under accession number SRX019580. Microarray data were submitted to EBI ArrayExpress under accession number E-MTAB-1960.

Supplemental Information

Supplemental Information includes Supplemental Experimental Procedures, six figures, two tables, and sequence and alignment data and can be found with this article online at <http://dx.doi.org/10.1016/j.cub.2013.12.003>.

Acknowledgments

We thank Antje Thomas for the help with microscopy, Thomas Walter for constructing jellyfish facility, and Elke Blohm-Sievers for the help with microarrays. Tatiana Shaposhnikova and Gerhard Jarms provided the animal lines. Ivan Gluzdikov, Ludmila Kuznetzova, and Rainer Herges gave important advice in organic chemistry. Ulrich Technau, Johanna Kraus, and David Fredman shared with us highly valuable unpublished *Clytia* and *Aurelia* data. We are grateful to Diethard Tautz for the opportunity to use research facilities at MPI for Evolutionary Biology in Plön. K.K. thanks Oleg Chaga, Ivan Tikhomirov, and Ivan Rudsky for inspiring discussions. Our work was financially supported by DFG Clusters "Future Ocean" and "Inflammation at Interfaces." K.K. is supported by RFBR (PФФИ) grant 13-04-01795. W.W. was supported by China Scholarship Council.

Received: May 2, 2013

Revised: August 19, 2013

Accepted: December 3, 2013

Published: January 16, 2014

References

- McBrayer, Z., Ono, H., Shimell, M., Parvy, J.P., Beckstead, R.B., Warren, J.T., Thummel, C.S., Dauphin-Villeman, C., Gilbert, L.I., and O'Connor, M.B. (2007). Prothoracicotropic hormone regulates developmental timing and body size in *Drosophila*. *Dev. Cell* 13, 857–871.
- Brown, D.D., and Cai, L. (2007). Amphibian metamorphosis. *Dev. Biol.* 306, 20–33.
- Laudet, V. (2011). The origins and evolution of vertebrate metamorphosis. *Curr. Biol.* 21, R726–R737.
- Hofmann, D.K., Neumann, R., and Henne, K. (1978). Strobilation, budding and initiation of scyphistoma morphogenesis in the rhizostome *Cassiopea andromeda* (Cnidaria, Scyphozoa). *Mar. Biol.* 47, 161–176.
- Leitz, T., and Wagner, T. (1993). The marine bacterium *Alteromonas espejiana* induces metamorphosis of the hydroid *Hydractinia echinata*. *Mar. Biol.* 115, 173–178.
- Kroiher, M., Siefker, B., and Berking, S. (2000). Induction of segmentation in polyps of *Aurelia aurita* (Scyphozoa, Cnidaria) into medusae and formation of mirror-image medusa anlagen. *Int. J. Dev. Biol.* 44, 485–490.
- Miyake, H., Terazaki, M., and Kakinuma, Y. (2002). On the polyps of the common jellyfish *Aurelia aurita* in Kagoshima Bay. *J. Oceanogr.* 58, 451–459.
- Collins, A.G. (2002). Phylogeny of Medusozoa and the evolution of cnidarian life cycles. *J. Evol. Biol.* 15, 418–432.
- Collins, A.G., Schuchert, P., Marques, A.C., Jankowski, T., Medina, M., and Schierwater, B. (2006). Medusozoan phylogeny and character evolution clarified by new large and small subunit rDNA data and an assessment of the utility of phylogenetic mixture models. *Syst. Biol.* 55, 97–115.
- Seipel, K., and Schmid, V. (2006). Mesodermal anatomies in cnidarian polyps and medusae. *Int. J. Dev. Biol.* 50, 589–599.
- Schmich, J., Trepel, S., and Leitz, T. (1998). The role of GLWamides in metamorphosis of *Hydractinia echinata*. *Dev. Genes Evol.* 208, 267–273.
- Müller, W.A. (1984). Retinoids and pattern formation in a hydroid. *J. Embryol. Exp. Morphol.* 81, 253–271.
- Kostrouch, Z., Kostrouchova, M., Love, W., Jannini, E., Piatigorsky, J., and Rall, J.E. (1998). Retinoic acid X receptor in the diploblast, *Tripedalia cystophora*. *Proc. Natl. Acad. Sci. USA* 95, 13442–13447.
- Kuniyoshi, H., Okumura, I., Kuroda, R., Tsujita, N., Arakawa, K., Shoji, J., Saito, T., and Osada, H. (2012). Indomethacin induction of metamorphosis from the asexual stage to sexual stage in the moon jellyfish, *Aurelia aurita*. *Biosci. Biotechnol. Biochem.* 76, 1397–1400.
- Möller, H. (1980). Population dynamics of *Aurelia aurita* medusae in Kiel Bight, Germany (FRG). *Mar. Biol.* 60, 123–128.
- Berking, S., Czech, N., Gerharz, M., Herrmann, K., Hoffmann, U., Raifer, H., Sekul, G., Siefker, B., Sommerer, A., and Vedder, F. (2005). A newly discovered oxidant defence system and its involvement in the development of *Aurelia aurita* (Scyphozoa, Cnidaria): reactive oxygen species and elemental iodine control medusa formation. *Int. J. Dev. Biol.* 49, 969–976.
- Schroth, W., Jarms, G., Streit, B., and Schierwater, B. (2002). Speciation and phylogeography in the cosmopolitan marine moon jelly, *Aurelia* sp. *BMC Evol. Biol.* 2, 1.
- Gudernatsch, J.F. (1912). Feeding experiments on tadpoles. I. The influence of specific organs given as food on growth and differentiation, a contribution to the knowledge of organs with internal section. *Arch. Entwicklungsmech. Org.* 35, 457–483.
- Furlow, J.D., and Neff, E.S. (2006). A developmental switch induced by thyroid hormone: *Xenopus laevis* metamorphosis. *Trends Endocrinol. Metab.* 17, 40–47.
- Wu, W., Niles, E.G., and LoVerde, P.T. (2007). Thyroid hormone receptor orthologues from invertebrate species with emphasis on *Schistosoma mansoni*. *BMC Evol. Biol.* 7, 150.
- Nakagawa, Y., and Henrich, V.C. (2009). Arthropod nuclear receptors and their role in molting. *FEBS J.* 276, 6128–6157.
- Song, J., Angel, A., Howard, M., and Dean, C. (2012). Vernalization - a cold-induced epigenetic switch. *J. Cell Sci.* 125, 3723–3731.
- Heggie, L., and Halliday, K.J. (2005). The highs and lows of plant life: temperature and light interactions in development. *Int. J. Dev. Biol.* 49, 675–687.
- Putnam, N.H., Srivastava, M., Hellsten, U., Dirks, B., Chapman, J., Salamov, A., Terry, A., Shapiro, H., Lindquist, E., Kapitonov, V.V., et al. (2007). Sea anemone genome reveals ancestral eumetazoan gene repertoire and genomic organization. *Science* 317, 86–94.
- Shinzato, C., Shoguchi, E., Kawashima, T., Hamada, M., Hisata, K., Tanaka, M., Fujie, M., Fujiwara, M., Koyanagi, R., Ikuta, T., et al. (2011). Using the *Acropora digitifera* genome to understand coral responses to environmental change. *Nature* 476, 320–323.
- Chapman, J.A., Kirkness, E.F., Simakov, O., Hampson, S.E., Mitros, T., Weinmaier, T., Rattei, T., Balasubramanian, P.G., Borman, J., Busam, D., et al. (2010). The dynamic genome of *Hydra*. *Nature* 464, 592–596.